RSC Advances


This is an *Accepted Manuscript*, which has been through the Royal Society of Chemistry peer review process and has been accepted for publication.

*Accepted Manuscripts* are published online shortly after acceptance, before technical editing, formatting and proof reading. Using this free service, authors can make their results available to the community, in citable form, before we publish the edited article. This *Accepted Manuscript* will be replaced by the edited, formatted and paginated article as soon as this is available.

You can find more information about *Accepted Manuscripts* in the Information for Authors.

Please note that technical editing may introduce minor changes to the text and/or graphics, which may alter content. The journal's standard Terms & Conditions and the Ethical guidelines still apply. In no event shall the Royal Society of Chemistry be held responsible for any errors or omissions in this *Accepted Manuscript* or any consequences arising from the use of any information it contains.

ROYAL SOCIETY OF CHEMISTRY

www.rsc.org/advances

Journal Name

RSCPublishing

COMMUNICATION

Cite this: DOI: 10.1039/x0xx00000x

# Hierarchical porous $Co_3O_4$@$Co_xFe_{3-x}O_4$ film as an advanced electrocatalyst for oxygen evolution reaction

Received 00th January 2012,
Accepted 00th January 2012

DOI: 10.1039/x0xx00000x

www.rsc.org/

Yaohang Gu*[a], Dandan Jia[a], Youshun Peng[a], Shitao Song[a], Yongguang Zhao[a], Jianping Zhang[a] and Dongjun Wang*[b]

**Fabricating a delicate structure for water oxidation is critical for developing high-efficient electrocatalysts which hold the significant situation for energy conversion devices. Herein we show an effective approach of constructing $Co_3O_4$@$Co_xFe_{3-x}O_4$ hierarchical nanostructure, which exhibits an obvious improvement for the eletrocatalytic activity relative to the $Co_xFe_{3-x}O_4$ nanoplates film and $Co_3O_4$ nanowires film. The enhancement is attributed to secondary $Co_xFe_{3-x}O_4$ nanoplates formed outside the $Co_3O_4$ nanowires, leading to a fantastic porous architecture and incorporating a more active electrocatalyst.**

The hierarchical nanostructured inorganic materials have been attracted the world-wide interests due to the unique physical and chemical properties.[1-5] Meanwhile, the growth the hierarchical nanostructures in a vertical fashion to form geometrically confined nano-array architectures has been identified as one of the most efficient routes to hugely boost the performances in various fields, including energy storage[6-8], sensors[9] and photoelectrochemical applications.[10, 11] Recently, the potential application of hierarchical nanostructures in electrochemical catalysis is investigated with superior performances[12-15], especially for oxygen evolution reaction(OER) which is a progress of generating oxygen through water oxidation, as this strategy will bring the following several advantages. Firstly, the oriented hierarchical nano-array architecture can offer a large contact surface area and high porosity, thus facilitating the ion diffusion.[16] Secondly, direct growth of active catalysts on conductive substrates can ensure good electric conductivity and mechanical adhesion, which accelerates the electron transport and stabilizes the surface morphology and structure.[17] Lastly, the nanostructured architecture was demonstrated to significantly reduce the releasing size of as-formed oxygen gas bubbles, thus offering a stable and fast current increase.[18]

Besides the structure designing, catalysts screening is equally crucial to achieve an excellent overall performance. Since 4 electrons are involved to generate one molecular oxygen, the kinetic of this reaction is relatively sluggish, thus huge overpotentials are required to drive this reaction.[19, 20] An effective electrocatalyst can obviously reduce the overpotential, thereby improving the energy efficiency. Up to date, the most active OER catalysts are $RuO_2$ and $IrO_2$[21, 22], but these two kinds of metal oxides are in the face of scarcity and high cost, which restrict it from large-scale usage. Alternatively, earth-abundant metals (Co, Ni, Fe, Mn) based compounds are discovered with comparable activities for OER.[23-28] In particular, $Co_3O_4$ is a typically active, stable and inexpensive catalyst in alkaline condition, as the Co has been identified as the active centre for OER.[29-31] Moreover, introducing other transition metals into the Co matrix was demonstrated with superior OER activity to either of the parent metal oxides due to the creation of new active sites with lower activation energy.[32] Therefore, we believe that mixed transition metal oxides are worthy to be explored due to their great potential in delivering outstanding OER activities.

Herein, we employed a three-step synthesis protocol to fabricate hierarchical porous $Co_3O_4$@$Co_xFe_{3-x}O_4$ thin film with $Co_3O_4$ nanowires as the core and mixed Co and Fe oxides nanoplates as the shell. It was found that the mixed oxides are derived from $Co_2(OH)_2CO_3$ and CoFe layer double hydroxide precursors (CoFe-LDH). The electrochemical results suggested that the hierarchical porous $Co_3O_4$@$Co_xFe_{3-x}O_4$ was a novel electrocatalyst material with high OER activity and stability in basic solutions, much better than those of the $Co_xFe_{3-x}O_4$ nanoplates film and $Co_3O_4$ nanowires film. The intrinsically high activity of $Co_3O_4$@$Co_xFe_{3-x}O_4$ and unique structure was believed to be responsible for the high electrocatalytic performance. This study not only provided a new and efficient OER catalyst, but also opened up a new opportunity for constructing advanced structures for next generation water splitting and metal-air battery devices.

The synthesizing process of hierarchical porous $Co_XFe_{3-X}O_4$ involved three steps which were shown in Fig. 1. We chose the

RSC Advances Accepted Manuscript

nickel foam as the substrate because of its high porosity and zigzag skeleton which endowed the film with a high surface area. The $Co_2(OH)_2CO_3$ nanowires were firstly grown on the nickel foam by a hydrothermal method. After that the CoFe layered double hydroxide nanoplates were in-situ constructed along the nanowire skeleton with a similar hydrothermal process as well. At last, the hierarchical porous $Co_3O_4$@$Co_xFe_{3-x}O_4$ was formed by a calcination process. The morphology evolution process was examined by scanning electron microscope (SEM), which manifested that $Co_2(OH)_2CO_3$ nanowires were uniformly grew on the substrate with a smooth surface (Fig. 2A and B) . After the secondly hydrothermal process, it was observed that a large amount of nanoplates grown outside the nanowire (Fig. S1). Each nanoplate was approximately 400 nm in length with a hexagonal shape and the calcinations process did not destroy the porous architecture (Fig. 2C-F). The energy dispersive spectroscopy results (EDS, Fig. S2) showed that the metal elements were uniformly distributed on the hierarchical porous structure with a molar ratio of ~1:1 for Co and Fe (Table S1).

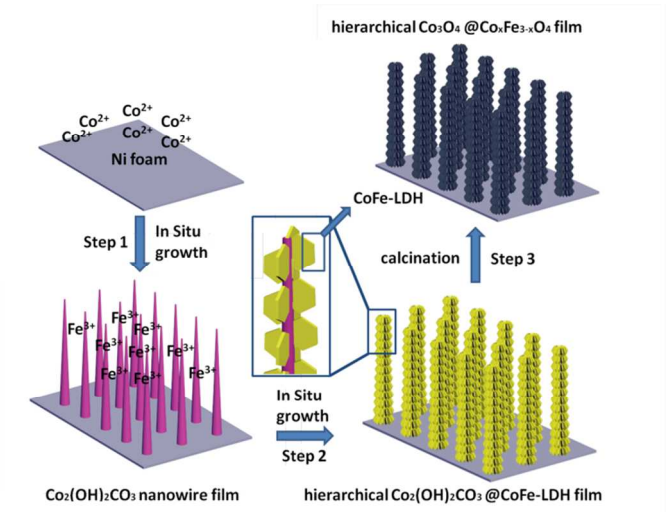


**Figure 1.** Schematic illustration of the fabrication process of hierarchical porous $Co_xFe_{3-x}O_4$ thin film grown on nickel foam.

The morphology evolution induced by the hydrothermal process usually brought about a phase transformation, which was revealed by the X-ray diffraction (XRD) patterns of all the precursors and final products. The red line in Fig. 3A demonstrated that the nanowires were mainly with $Co_2(OH)_2CO_3$ phase (JCPDF: 48-0083), which was then converted into $Co_3O_4$ phase (JCPDF: 42-1467) by the calcinations process (black line, the peaks marked "#" denoted the Ni substrate). Figure 3B revealed that, after the second-step growth, a serious of CoFe-LDH reflections (red line) was observed in addition to the $Co_2(OH)_2CO_3$ phase, demonstrating a successful transformation from a orthorhombic structure to layered hexagonal structure. The final product (black line) showed a spinel structure which can be attributed to the $CoFe_2O_4$ reflection (JCPDF: 03-0864), while the slightly shifted positions might result from the variation ratio between Co and Fe.[33-35] The X-ray photoelectron spectroscopy (XPS, Fig. S3) results further confirmed the existence of both elements in the porous film with the oxidation states of +2 and +3 for Co and Fe, respectively.

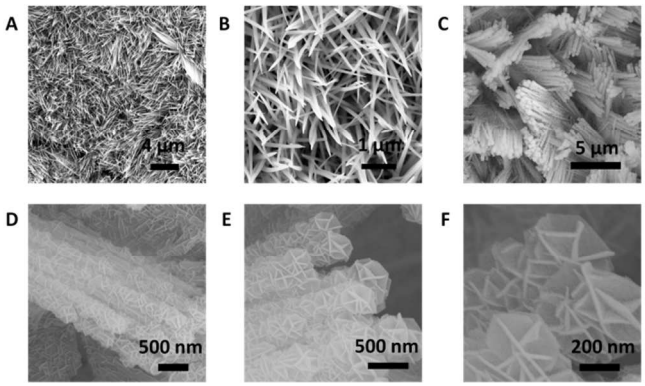


**Figure 2.** (A) and (B), SEM images of $Co_3O_4$ nanowires film with different magnifications; (C), (D), (E) and (F), SEM images of $Co_3O_4$@$Co_xFe_{3-x}O_4$ hierarchical nanostructure with different magnifications.

In order to gain more structural information, transmission electron microscope (TEM) and high resolution transmission electron microscope (HRTEM) were employed, as shown in Fig. 4. The TEM image clearly showed that the hexagonal nanoplates were grew outside the $Co_3O_4$ nanowire backbone (Fig. 4A), in consistent with the SEM images. HRTEM result (Fig. 4B) further confirmed a core-shell structure and the observed lattice spacings matched well with a spinel-type structure.

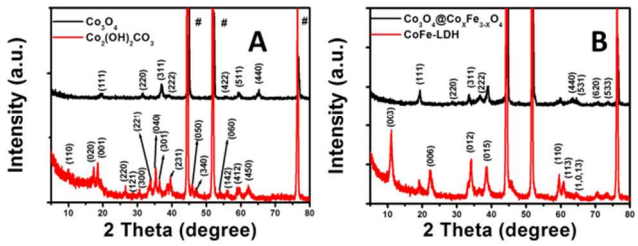


**Figure 3.** XRD patterns of as-prepared samples: (A) The $Co(OH)_2CO_3$ (red) and the obtained $Co_3O_4$ after calcinations (black); (B) the CoFe-LDH (red) and the obtained hierarchical porous $Co_3O_4$@$Co_xFe_{3-x}O_4$ (black).

The formation mechanism of CoFe-LDH outside of the $Co_2(OH)_2CO_3$ nanowires can be interpreted by the dissolution and co-precipitation of $Co^{2+}$ and $Fe^{3+}$ ions. Since the pH value of the precursor solution containing $FeCl_3$ and HCl was below 2, the Co was not stable and it might be dissolved.[32, 36] The prolonging of the reaction time would result in the substitution of $Co^{2+}$ to the $Fe^{3+}$. And the gradual hydrolysis of $Fe^{3+}$ and $Co^{2+}$ would resulting in the LDH formation associated with existed $CO_3^{2-}$ in $Co_2(OH)_2CO_3$ nanowires as the intercalation anion.

RSC Advances Accepted Manuscript


This journal is © The Royal Society of Chemistry 2012

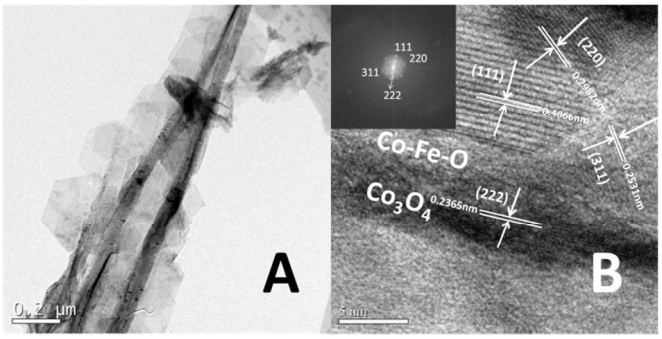


**Figure 4.** Hierarchical porous $Co_XFe_{3-X}O_4$ thin film of (A) typical TEM image; (B) typical HRTEM image (inset is FFT).

Such a hierarchical porous film would benefit the electrochemical reactions on the electrode surface in virtue of the enlarged surface area and abundant active sites. Here we evaluated the OER activity of the hierarchical $Co_3O_4$@$Co_xFe_{3-x}O_4$ film using a typical three-electrode setup in $O_2$-saturated 1 M KOH electrolyte. The $Co_xFe_{3-x}O_4$ nanoplates film (SEM, EDS and XRD results can be seen in Fig. S4) and $Co_3O_4$ nanowires film were also tested as a control sample. Polarization curves demonstrated the hierarchical $Co_3O_4$@$Co_xFe_{3-x}O_4$ film exhibited an onset potential (Fig. 5A, defined as the start point in the linear range of Tafel slope) of ~1.54 V vs. RHE and an overpotential of ~390 mV at ~150 mA $cm^{-2}$ ($\eta_{150}$). On the contrary, the $Co_xFe_{3-x}O_4$ nanoplates film showed a similar onset potential (~1.54 V), but the OER current increase was much slower, leading to a higher overpotential (~437 mV) for achieving ~150 mA $cm^{-2}$. For the $Co_3O_4$ nanowires film, the onset potential was only ~1.59 V with an $\eta_{150}$ value of ~510 mV, demonstrating that the secondary formed $Co_xFe_{3-x}O_4$ was a more active electrocatalyst for OER. To gain more insight into the OER activity, Tafel plots derived from polarization curves were constructed (Fig. 5B). The resulting Tafel slope of hierarchical $Co_3O_4$@$Co_xFe_{3-x}O_4$ film was ~53 mV $dec^{-1}$, which was similar to the $Co_xFe_{3-x}O_4$ nanoplates film but much smaller than that of $Co_3O_4$ nanowires film (~96 mV $dec^{-1}$), indicating that the formation of $Co_xFe_{3-x}O_4$ was benefit for accelerating the OER kinetics.[37, 38]

The surface area of 3 samples ($Co_3O_4$ nanowires film, hierarchical $Co_3O_4$@$Co_xFe_{3-x}O_4$ film and $Co_xFe_{3-x}O_4$ nanoplates film) were also tested by both BET testing and electrochemical testing, as shown in Fig. 5C-E, and Fig. S5. The BET result revealed that the hierarchical $Co_3O_4$@$Co_xFe_{3-x}O_4$ film showed the highest surface area with a value of 0.689 $m^2$ $cm^{-2}$, much higher than those of two counterparts (0.466 $m^2$ $cm^{-2}$ for $Co_xFe_{3-x}O_4$ nanoplates film and 0.389 $m^2$ $cm^{-2}$ for $Co_3O_4$ nanowires film). The electrochemical results were in good accordance with the BET results. A high double layer capacitance (~171.76 mF $cm^{-2}$) was observed for the hierarchical $Co_3O_4$@$Co_xFe_{3-x}O_4$ film, corresponding to a roughness factor of ~2862.[39] On the contrary, the $Co_3O_4$ nanowires film and $Co_xFe_{3-x}O_4$ nanoplates film showed much inferior electrochemical surface areas (~82.79 mF $cm^{-2}$ and ~90.16 mF $cm^{-2}$ for $Co_xFe_{3-x}O_4$ nanoplates film and $Co_3O_4$ nanowires film, respectively), further demonstrating the effectiveness of hierarchical construction on improving the porosity of the materials.

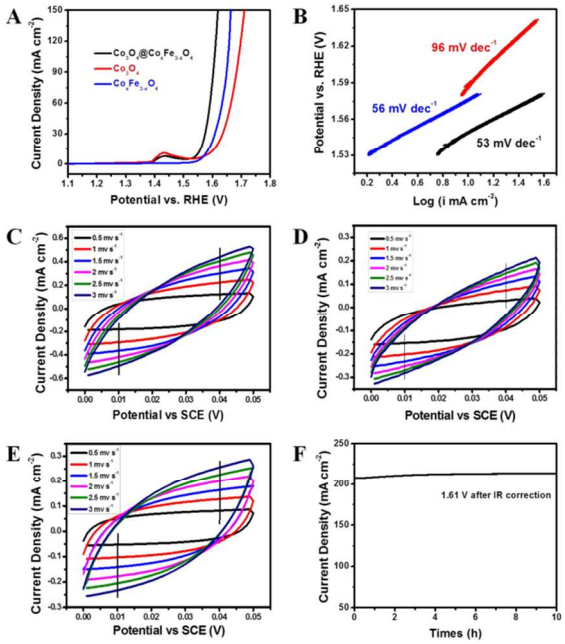


**Figure 5.** (A), polarization curve of the hierarchical $Co_3O_4$@$Co_xFe_{3-x}O_4$ film (black line), $Co_xFe_{3-x}O_4$ nanoplates film (blue line) and $Co_3O_4$ nanowire film (red line); (B), Tafel plots of samples (black line: $Co_3O_4$@$Co_xFe_{3-x}O_4$ film; blue line: $Co_xFe_{3-x}O_4$; red line: $Co_3O_4$). (C), (D) and (E), electrochemical surface area (ESA) measurements of the hierarchical $Co_3O_4$@$Co_xFe_{3-x}O_4$ film, $Co_xFe_{3-x}O_4$ nanoplates film and $Co_3O_4$ nanowire film respectively; (F), Stability result of the hierarchical $Co_3O_4$@$Co_xFe_{3-x}O_4$ film at a high current density, the applied potential is 1.61 V after IR correction.

The long-term stability of a catalytic electrode is another critical issue to consider for commercial applications. In this case, a high and stable current density (>200 mA $cm^{-2}$) with negligible degradation for 10 h was observed for the hierarchical $Co_3O_4$@$Co_xFe_{3-x}O_4$ film (Fig. 5F), indicating a prominent stability at a constant applied potential. Combination of the above features (small overpotential and high durability) validated the hierarchical $Co_3O_4$@$Co_xFe_{3-x}O_4$ film as an advanced and promising OER electrode.

We attributed the significantly enhanced OER performance to the secondary formed $Co_xFe_{3-x}O_4$ nanoplates, which act as a more active electrocatalyst for OER and result in the formation of a highly porous hierarchical structure. It is observed that the hierarchical $Co_3O_4$@$Co_xFe_{3-x}O_4$ film showed a high intrinsic OER activity (a low onset potential of ~1.54 V and a small Tafel slope value of ~53 mV $dec^{-1}$), similar to the $Co_xFe_{3-x}O_4$ nanoplates film but much higher than that of the pure $Co_3O_4$ nanowires film, indicating that the introduction of Fe element into Co matrix would lead to the great enhancement on the intrinsic OER activity. Co is generally considered as the active center for OER because of its suitable binding energy (not too strong not too weak) to oxygen intermediates, and moreover, a latest literature also reported that Fe-doped $Co_3O_4$ replica could show a much enhanced OER activity than pure $Co_3O_4$, which was attributed to the formation of spinel phased

RSC Advances Accepted Manuscript

$CoFe_2O_4$. The different electronic structure of the material might affect the conductivity and charge transferability, thereby influencing the OER activity.[32, 40] Therefore, it is reasonable that $Co_xFe_{3-x}O_4$ derived from CoFe-LDH is a potential electro-catalyst for water oxidation.

More importantly, the unique hierarchical architecture should be another essential role for the enhanced OER performance. Compared with the nanowires film, the hierarchical structures can offer an even higher surface area and porosity, while the conductivity can be well preserved.[15, 41] The hierarchical porosity could accelerate the diffusion of the $OH^-$ ions, which accelerated the kinetics. Therefore, the improved OER performance of the hierarchical $Co_3O_4@Co_xFe_{3-x}O_4$ film could be easily understood by a combination of inducing a more active electro-catalyst and constructing a hierarchical architecture at the electrode surface.

In summary, we have developed a facile and cost-effective method to fabricate a hierarchical $Co_3O_4@Co_xFe_{3-x}O_4$ film with mixed Co and Fe oxides as the shell and $Co_3O_4$ as the core on Ni foam. This hierarchical film can offer a large surface area, high porosity and good conductivity, which are all beneficial in promoting the surface electrochemical reactions. As an example, the hierarchical $Co_3O_4@Co_xFe_{3-x}O_4$ film exhibited a significantly enhanced OER performance relative to the $Co_xFe_{3-x}O_4$ nanoplates film and $Co_3O_4$ nanowires film. It is found that the highly active $Co_xFe_{3-x}O_4$ nanoplates and the 3D porous structure are responsible for the high OER performance. This work provides a propitious route for designing low cost, high performance and scalable OER electrodes, which act as a necessary component for water splitting and metal air battery aiming at achieving maximum market penetration of intermittent renewable energy.

This work was supported by the Nature Science Foundation of Hebei Province (E2013407124), the Education Department of Hebei Province (ZH2012039, Z2010258).

## Notes and references

[a] Department of Chemical Engineering, Hebei Normal University of Science and Technology, West Hebei Street, Qin Huangdao 066000, China
Tel.: +86-10-13133519996
E-mail: guyaohang@163.com
[b] Department of Instruments and Analysis, Hebei Normal University of Science and Technology, West Hebei Street, Qin Huangdao 066000, China
Tel.: +86-10-18603362011
E-mail: wdj9999@126.com
Electronic Supplementary Information (ESI) available: [experimental section, XPS survey, mapping data results]. See DOI: 10.1039/c000000x/

1.L. Jing, W. Zhou, G. Tian and H. Fu, *Chem. Soc. Rev.*, 2013, **42**, 9505-9549.
2. A. I. Hochbaum and P. Yang, *Chem. Rev.*, 2009, **110**, 527-546.
3. L. Mai, X. Tian, X. Xu, L. Chang and L. Xu, *Chem. Rev.*, 2014, **DOI: 10. 1021/cr500177a**.
4. R. Subbaraman, D. Tripkovic, K. Chang, D. Strmcnik, A. P. Paulikas, P. Hirunsit, M. Chan, J. Greeley, V. Stamenkovic and N. M. Markovic, *Nat. Mater.*, 2012, **11**, 550-557.
5. Y. Yang, G. zheng and Y. Cui, *Chem. Soc. Rev.*, 2013, **42**, 3018-3032.
6. S. Zhou, X. Yang, Y. Lin, J. Xie and D. Wang, *ACS Nano.*, 2012, **6**, 919-924.
7. F. Fabregat-Santiago, E. M. Barea, J. Bisquert, G. K. Mor, K. Shankar and C. A. Grimes, *J. Am. Chem. Soc.*, 2008, **130**, 11312-11316.
8. Q. Yang, Z. Lu, Z. Chang, W. Zhu, J. Sun, J. Liu, X. Sun and X. Duan, *RSC Adv.*, 2011, **1**, 1-6.
9. K. Ariga, Q. Ji, M. J. McShane, Y. M. Lvov, A. Vinu and J. P. Hill, *Chem. Mater.*, 2012, **24**, 728-737.
10. R. D. L. Smith, M. S. Prevot, R. D. Fagan, Z. Zhang, P. A. Sedach, M. K. J. Siu, S. Trudel and C. P. Berlinguette, *Science*, 2013, **340**, 60-63.
11. B. Klahr, S. Gimenez, F. Fabregat-Santiago, J. Bisquert and T. W. Hamann, *J. Am. Chem. Soc.*, 2012, **134**, 16693-16700.
12. G. Du, X. Liu, Y. Zong, T. S. A. Hor, A. Yu and Z. Liu, *Nanoscale*, 2013, **5**, 4657-4661.
13. F. Lu, X. Cao, Y. Wang, C. Jin, M. Shen and R. Yang, *RSC adv.*, 2014, **4**, 40373-40376.
14. Y. Cao, Z. Wei, J. He, J. Zhang, Q. Zhang, M. Zheng and Q. Dong, *Energy Environ. Sci.*, 2012, **5**, 9765-9768.
15. Y. Li, P. Hasin and Y. Wu, *Adv. Mater.*, 2010, **22**, 1926-1929.
16. J. B. Gerken, J. G. McAlpin, J. Y C. Chen, M. L. Rigsby, W. H. Casey, R. D. Britt and S. S. Stahl, *J. Am. Chem. Soc.*, 2011, **133**, 14431-14442.
17. J. Wang, H. Zhong, Y. Qin and X. Zhang, *Angew. Chem. Int. Ed.*, 2013, **52**, 1-6.
18. Z. Lu, W. Zhu, X. Yu, H. Zhang, Y. Li, X. Sun, X. Wang, H. Wang, J. Wang and J. Luo, *Adv. Mater.*, 2014, **26**, 2683-2687.
19. A. Bergmann, I. Zaharieva, H. Dau and P. Strasser, *Energy Environ. Sci.*, 2013, **6**, 2745-2755.
20. I. C. Man, H. Y. Su, F. Calle-Vallejo, H. A. Hansen, J. I. Martinez, N. G. Inoglu, J. Kitchin, T. F. Jaramillo, J. K. Norskov and J. Rossmeis, *ChemCatChem.*, 2011, **3**, 1159-1165.
21. H. G. Jung, Y. S. Jeong, J. B. Park, Y. K. Sun, B. Scrosati and Y. J. Lee, *ACS Nano*, 2013, **7**, 3532-3539.
22. J. Xu, D. Aili, Q. Li, E. Christensen, J. O. Jensen, W. Zhang, M. K. Hansen, G. Liu, X. Wang and N. J. Bjerrum, *Energy Environ. Sci.*, 2014, **7**, 820-830.
23. E. L. Miller and R. E. Rocheleau, *J. Electrochem. Soc.*, 1997, **144**, 3072-3076.
24. M. Gong, Y. Li, H. Wang, Y. Liang, J. Z. Wu, J. Zhou, J. Wang, T. Regier, F. Wei and H. Dai, *J. Am. Chem. Soc.*, 2013, **135**, 8452-8455.
25. M. S. El-Deab, M. I. Awad, A. M. Mohammad and T. Ohsaka, *Electrochem. Commun.*, 2007, **9**, 2082-2087.
26. M. E. Lyons and M. P. Brandon, *J. Electroanal. Chem.*, 2010, **641**, 119-130.
27. N. H. Chou, P. N. Ross, A. T. Bell and T. D. Tilley, *ChemSusChem.*, 2011, **4**, 1566-1569.
28. B. Cui, H. Lin, J.-B. Li, J. Yang and J. Tao, *Adv. Funct. Mater.*, 2008, **18**, 1440-1447.
29. H. Tuysuz, Y. J. Hwang, S. B. Khan, A. M. Asiri and P. Yang, *Nano. Res.*, 2013, **6**, 47-54.

RSC Advances Accepted Manuscript

 This journal is © The Royal Society of Chemistry 2012

30. J. A. Koza, Z. He, A. S. Miller and J. A. Switzer, *Chem. Mater.*, 2012, **24**, 3567-3573.
31. G. Zhao, Z. Xu and K. Sun, *J. Mater. Chem. A*, 2013, **1**, 12862-12867.
32. T. Grewe, X. Deng and H. Tuysuz, *Chem. Mater.*, 2014, **26**, 3162-3168.
33. J. Sun, Y. Li, X. Liu, Q. Yang, J. Liu, X. Sun, D. G. Evans and X. Duan, *Chem. Commun.*, 2012, **48**, 3379-3381.
34. Q. Q. Xiong, X. H. Xia, J. P. Tu, J. Chen, Y. Q. Zhang, D. Zhou, C. D. Gu and X. L. Wang, *J. Power Sources*, 2013, **240**, 344-350.
35. Y. N. Ko, S. B. Park, J.-H. Lee and Y. C. Kang, *RSC Adv.*, 2014, **4**, 40188-40192.
36. Y. Meng, D. Chen and X. Jiao, *J. Phys. Chem. B.*, 2006, **110**, 15212-15217.
37. E. B. Castro and C. A. Grevasi, *Int. J. Hydrogen. Energ.*, 2000, **25**, 1163-1170.
38. E. B. Castro, C. A. Grevasi and J. R. Vilche, *J. Appl. Electrochem.*, 1998, **28**, 835-841.
39. Q. Yang, Z. Lu, X. Sun and J. Liu, *Sci. Rep.*, 2013, **3**, 3537.
40. Z. Lu, H. Wang, D. Kong, K. Yan, P.-C. Hsu, G. Zheng, H. Yao, Z. Liang, X. Sun and Y. Cui, *Nat. Commun.*, 2014, **5**, 4345-4351.
41. B. Lu, D. Cao, P. Wang, G. Wang and Y. Gao, *Int. J. Hydrogen. Energ.*, 2011, **36**, 72-78.

RSC Advances Accepted Manuscript